

Large is different: non-monotonic behaviour of elastic range scaling in polymeric turbulence at large Reynolds and Deborah numbers

Marco E. Rosti,^{1,*} Prasad Perlekar,² and Dhruvaditya Mitra³

¹*Complex Fluids and Flows Unit, Okinawa Institute of Science and Technology Graduate University, 1919-1 Tancha, Onna-son, Okinawa 904-0495, Japan*

²*TIFR Centre for Interdisciplinary Sciences, Tata Institute of Fundamental Research, Gopanpally, Hyderabad 500046, India.*

³*Nordita, KTH Royal Institute of Technology and Stockholm University, Roslagstullsbacken 23, 10691 Stockholm, Sweden*

We use high resolution direct numerical simulations to study statistically stationary, homogeneous, and isotropic turbulent flows of dilute solutions of polymers at high Reynolds numbers and Deborah numbers. We find that for small wavenumbers k , the kinetic energy spectrum shows Kolmogorov-like behavior which crosses over at a larger k to a novel, elastic scaling regime, $E(q) \sim k^{-\xi}$, with $\xi \approx 2.3$, providing support to and extending the analysis of recent experimental results [1]. We uncover the mechanism of elastic scaling by studying the contribution of the polymers to the flux of kinetic energy through scales. The contribution can be decomposed into two parts: one, expected, increase in effective viscous dissipation of the flow and two, a purely elastic contribution that dominates over the nonlinear flux in the range of k over which the elastic scaling is observed. The multiscale balance between the two fluxes determines the crossover wavenumber which, intriguingly, depends non-monotonically on the Deborah number. The probability distribution function of polymer extension also depends non-monotonically on the Deborah number. Consistent with this picture, real space structure functions also show two scaling ranges, with intermittency present in both of them in equal measure.

I. INTRODUCTION

Since the discovery of turbulent drag reduction by Toms [2], turbulent flows with small amount of long-chained polymers have remained an exciting field of research. In addition to polymer concentration, two dimensionless numbers, the Reynolds number and the Deborah number, are necessary to describe such a turbulent flow. The former estimates the importance of the inertial term in the Navier–Stokes equation compared to the viscous term, and the latter is the ratio of the characteristic time scale of the polymers over the typical time scale of the large scale eddies in the turbulent flow. The turbulent drag reduction appears at both large Reynolds and Deborah. Evidently it is not possible to study drag reduction in homogeneous and isotropic turbulent flows, nevertheless such flows are studied, since the pioneering work by Tabor and De Gennes [3], in search of deeper insights.

The elementary effect of the addition of polymers to a fluid is an increase in the effective viscosity of the solution [4, 5]. Nevertheless, there can be net reduction of the dissipation of kinetic energy [6–12] because the presence of polymers changes the turbulent cascade *qualitatively*. Significant theoretical [3, 5, 13–15], numerical [9, 11, 12, 16–27], and experimental [1, 6, 28–33] efforts have gone into elucidating the nature of the turbulent energy cascade in the presence of polymers. It is now reasonably well established [9, 11] that for large enough scale separation between the energy injection scale, L_{inj} , and the Kolmogorov scale, L_K , there exists an intermediate scale L_p such that for scales $L_p < r < L_{\text{inj}}$ the

energy cascade is practically the same as that of a Newtonian flow, with the shell-integrated energy spectrum being $E(k) \sim k^{-5/3}$ and the second order structure function $S_2(r) \sim r^{2/3}$. For scales r such that $L_K < r < L_p$, energy is transferred from the fluid to the polymers and the kinetic energy spectrum is steeper than the Kolmogorov spectrum or in other words the second order structure function increases faster with r than $r^{2/3}$. Using the concept of scale-dependent Reynolds number [34], we may identify the flow at scale $r \ll L_p$ (also valid for $r < L_K$) with elastic turbulence – random viscoelastic smooth flows at very small Reynolds number. The spectrum for elastic turbulence is expected to be $E(k) \sim k^{-\xi}$ with $\xi > 3$ [15, 35, 36]. Is there a new scaling range for $r > L_p$ over which $S_2(r) \sim r^{\zeta_2}$ with $2/3 < \zeta_2 < 2$? This question could not be probed with the low-Reynolds and low-Deborah simulations quoted above. Recent experiments [1] had tentatively suggested that a new scaling range indeed appears, although the evidence is not yet unequivocal. Experiments [1, 37] also showed that, contrary to Lumley’s arguments [38], the scale L_p does depends on concentration of polymers.

Here we present evidence, from the highest resolution simulations of polymeric fluids, that indeed there is a range of scales r over which the structure function $S_2(r)$ seems to show scaling consistent with recent experimental results[1]. We also show that the new scaling is a purely elastic effect, and that this elastic behaviour is non-monotonic in Deborah number.

* marco.rosti@oist.jp

II. RESULTS

A. Governing equations

We use direct numerical simulations to study homogeneous isotropic turbulence with polymers [4, 39–43]. These are represented by a second rank tensor, \mathcal{C} with components $C_{\alpha\beta}$, which emerges as the thermal average of the tensor-product of the polymer end-to-end distance with itself. The polymer molecules are assumed to have a single relaxation time τ_p . The dynamical equations are:

$$\rho_f \left(\frac{\partial u_\alpha}{\partial t} + \frac{\partial u_\alpha u_\beta}{\partial x_\beta} \right) = -\frac{\partial p}{\partial x_\alpha} + \frac{\partial}{\partial x_\beta} \left(2\mu_f S_{\alpha\beta} + \frac{\mu_p}{\tau_p} f C_{\alpha\beta} \right) + \rho_f F_\alpha, \quad (1a)$$

$$\frac{\partial C_{\alpha\beta}}{\partial t} + u_\beta \frac{\partial C_{\alpha\beta}}{\partial x_\beta} = C_{\alpha\gamma} \frac{\partial u_\beta}{\partial x_\gamma} + C_{\gamma\beta} \frac{\partial u_\alpha}{\partial x_\alpha} - \frac{f C_{\alpha\beta} - \delta_{\alpha\beta}}{\tau_p}, \quad (1b)$$

$$\frac{\partial u_\alpha}{\partial x_\alpha} = 0. \quad (1c)$$

Here \mathbf{u} is the velocity, ρ_f and μ_f are the density and dynamic viscosity of the fluid, p is the pressure, μ_p is the polymer viscosity, and \mathcal{S} is the rate-of-strain tensor with components $S_{\alpha\beta}$ defined as $S_{\alpha\beta} = (\partial u_\alpha / \partial x_\beta + \partial u_\beta / \partial x_\alpha) / 2$. The function f is equal to unity ($f = 1$) in the purely elastic Oldroyd-B model, and to $f = (\mathcal{L}^2 - 3) / (\mathcal{L}^2 - C_{\gamma\gamma})$ in the FENE-P model (\mathcal{L} is the maximum polymer extensibility) exhibiting both shear-thinning and elasticity. Turbulence is sustained by the external force in the momentum equation, \mathbf{F} ; we use the spectral scheme from Eswaran and Pope [44] to randomly inject energy within a low-wavenumber shell with $k_{\text{inj}} = (1 \leq k \leq 2)$. In the statistically stationary state of turbulence, the injected energy is dissipated by both the fluid (ε_f) and the polymers (ε_p), thus $\varepsilon_{\text{inj}} = \varepsilon_f + \varepsilon_p$, where

$$\varepsilon_f = \frac{2\mu_f}{\rho_f} \langle S_{\alpha\beta} S_{\alpha\beta} \rangle, \quad \varepsilon_p = \frac{\mu_p}{\rho_f \tau_p} \langle f C_{\mu\mu} - 3 \rangle. \quad (2)$$

To compare, we also solve for the Navier–Stokes equations without any polymer additive – we call this the Newtonian simulation.

B. Theoretical background

Let us briefly recall essential features of fluid turbulence without polymeric additives [45]. The flow is determined by one dimensionless number, $\text{Re} = u_{\text{rms}} / (k_{\text{inj}} \nu_f)$, where u_{rms} is the root-mean-square velocity and $\nu_f = \mu_f / \rho_f$ is the kinematic viscosity of the fluid. Turbulent flows possess a range of length scales and corresponding time scales with strongly non-Gaussian statistics measured by the scaling exponents, ζ_q of the q -th order structure functions, S_q , of the longitudinal velocity differences,

$\delta u(\ell)$, over the length scale ℓ , defined by:

$$\delta u(\ell) \equiv [\mathbf{u}(\mathbf{x} + \boldsymbol{\ell}) - \mathbf{u}(\mathbf{x})] \cdot \left(\frac{\boldsymbol{\ell}}{\ell} \right), \quad (3a)$$

$$S_q(\ell) = \langle \delta u(\ell)^q \rangle \sim \ell^{\zeta_q}. \quad (3b)$$

Here $\langle \cdot \rangle$ denotes averaging over the statistically stationary state of turbulence. The q -th order structure function is the q -th order moment of the probability distribution function of velocity difference across a length scale ℓ . The scaling behavior of the structure function, (3b), holds for $\eta \ll \ell \ll L$ where $\eta \equiv (\nu_f^3 / \varepsilon_{\text{inj}})^{1/4}$ is called the viscous scale and L is called the integral scale. In practice, L is of the same order of $L_{\text{inj}} = 2\pi / k_{\text{inj}}$ and we will use them interchangeably. The non-Gaussianity is observed in two ways. First, the odd-order structure functions are non-zero, in particular the third order structure function satisfies the only known exact relation in turbulence – the four-fifth law – $S_3(\ell) = -(4/5)\varepsilon_{\text{inj}}\ell$. Second, the scaling exponents ζ_q are a nonlinear convex function of q – a phenomena called *intermittency*. The shell-integrated energy spectrum in Fourier space

$$E(k) \equiv \int_{|\mathbf{k}|=k} d^3\mathbf{k} \langle \hat{u}(\mathbf{k}) \hat{u}(-\mathbf{k}) \rangle, \quad (4)$$

where $\hat{u}(\mathbf{k})$ is the Fourier transform of the velocity field $\mathbf{u}(\mathbf{x})$, is itself the Fourier transform of the second order structure function $S_2(\ell)$. The theory of Kolmogorov gives $\zeta_q = q/3$ and consequently $E(k) \sim k^{-5/3}$, when k lies within the *inertial range*, $k_{\text{inj}} \ll k \ll k_\eta$, with $k_\eta \sim 1/\eta$.

In presence of polymers, we have, in addition, a contribution to the shell-integrated energy from the polymers, given by

$$E_p(k) \equiv \int_{|\mathbf{k}|=k} d^3\mathbf{k} \langle \hat{B}_\mu(\mathbf{k}) \hat{B}_\mu(-\mathbf{k}) \rangle, \quad (5)$$

where the matrix \mathcal{B} with components, $B_{\mu\nu}$, is the (unique) positive symmetric square root of the matrix \mathcal{C} , i.e., $C_{\alpha\beta} = B_{\alpha\mu} B_{\mu\beta}$ [25, 46]. The presence of polymers introduces also a new dimensionless number which is a ratio of the polymeric time scale τ_p over a characteristic time scale of the flow. As the turbulent flow has many time scales, it is common to define the Deborah number $\text{De} \equiv \tau_p / \tau_L$, where $\tau_L = L / u_{\text{rms}}$ is the large-eddy-turnover-time, and the Weissenberg number $\text{Wi} \equiv \tau_p / \tau_\eta$ where $\tau_\eta = \eta^2 / \nu$ [47].

In Fig. (1) we show typical pseudocolor plots of vorticity from Newtonian and viscoelastic simulations. The flow is qualitatively strongly affected by the presence of polymers, and small-scale vorticity structures are smoothed by the presence of the polymers, as can be seen by comparing Fig. (1A) and Fig. (1B), see also Ref. [9, 11, 18]. Surprisingly, as the Deborah number is increased beyond unity, this qualitative trend is reversed, compare Fig. (1B) and Fig. (1C). In Fig. (1C) small scale structures in vorticity reappears but at the same time we still find elongated structures although their length scales are smaller than their counterparts in Fig. (1B).

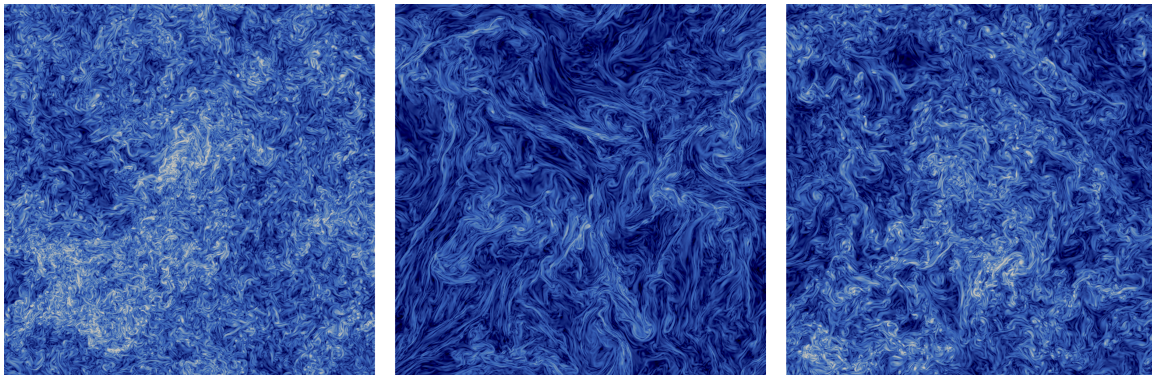


FIG. 1. **Instantaneous snapshots of the turbulent flows.** (left) Newtonian and viscoelastic fluid with (middle) $De \approx 1$ and (right) $De \approx 25$. The color contour shows the magnitude of the vorticity field, with the color-scale going from 0 (blue) to the maximum (white).

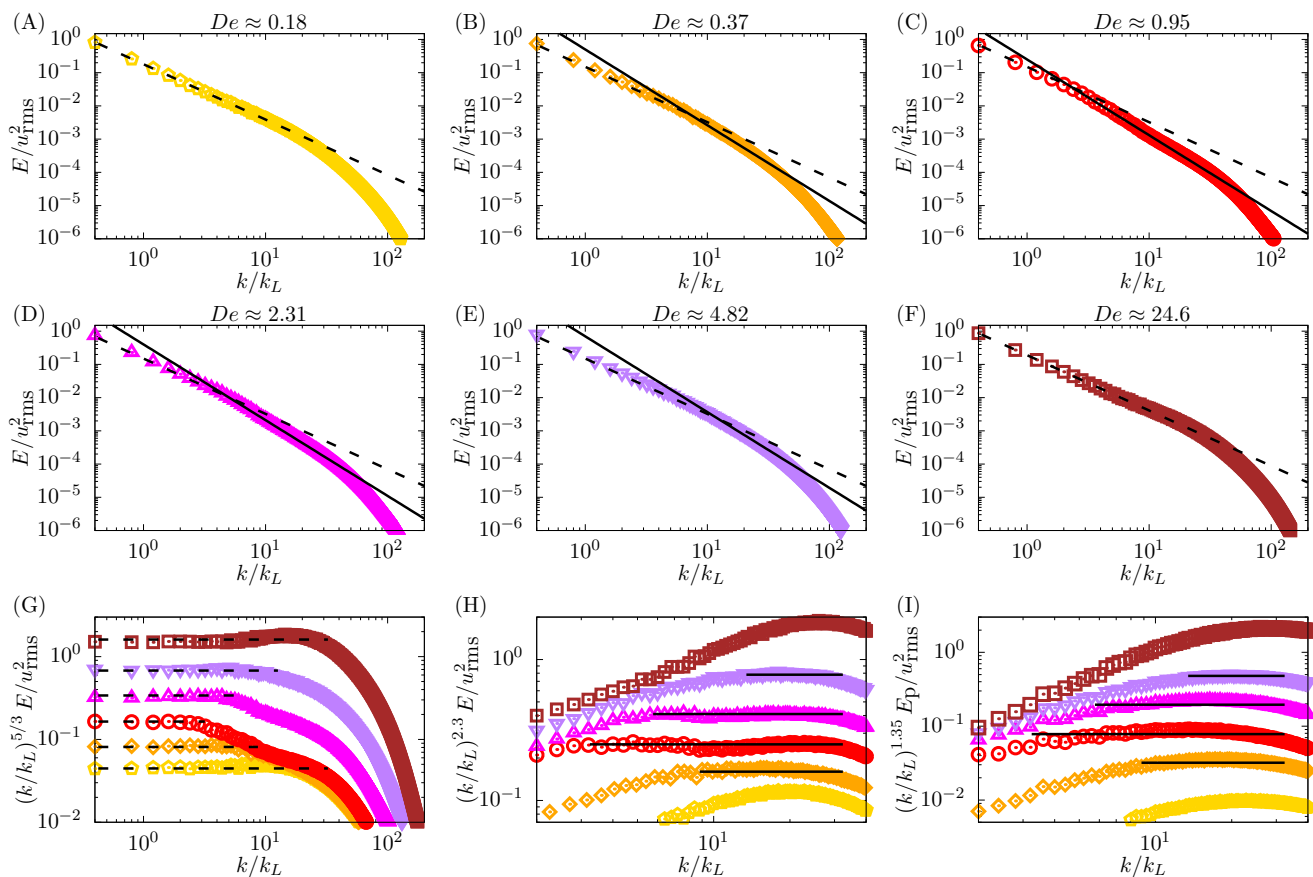


FIG. 2. **Kinetic and polymer energy spectra.** (A) to (F): Energy spectra for different Deborah numbers showing how the elastic range changes with De . (G) and (H): Compensated kinetic energy spectra showing the emergence of two scaling regions, Kolmogorov ($-5/3$) and elastic (-2.3) scaling respectively. In all the previous panels, the dashed and solid lines represent the $-5/3$ and -2.3 scalings. (I): Compensated polymer energy spectra for different Deborah numbers. The solid line represent the scaling $k^{-\psi}$ with $\psi \approx 1.35$.

C. Kinetic and polymer energy spectra

In Fig. (2) we plot the turbulent kinetic energy $E(k)$ for several values of Deborah number De . For the small Deborah numbers, e.g. $De \approx 0.18$, we observe, practi-

cally, the same behavior as Kolmogorov turbulence, with $E(k) \sim k^{-5/3}$ for the inertial range. As the Deborah number increases the range over which the Kolmogorov scaling is valid shrinks to smaller k , and at intermediate k a new range over which $E(k) \sim k^{-\xi}$ with $\xi \approx 2.3$

emerges. We call this new scaling range the *elastic range*. The spectra, in general, has three characteristic length scales (or equivalently wavenumbers). The largest is the one where energy is injected by stirring, the integral scale, $L \approx L_{\text{inj}}$. Next is the scale at which the Kolmogorov scaling crosses over to elastic scaling, L_p (corresponding wavenumber $k_p = 2\pi/L_p$). Last is the scale at which elastic scaling crosses over to the dissipative range, which we call the dissipative scale η (corresponding wavenumber $k_\eta = 1/\eta$). The Kolmogorov scaling is observed over the range $k_{\text{inj}} < k < k_p$ and the elastic range over the wavenumber range $k_p < k < k_\eta$. The elastic range spans over the maximum range of wavenumber for $\text{De} \approx 1$; as De is increased further the elastic range begins to shrink and the Kolmogorov range begins to grow again. Eventually, the elastic range practically disappears at $\text{De} \approx 5$ – the classical Kolmogorov range is restored. This remarkable behavior is better elucidated by plotting the two compensated spectra $k^{5/3}E(k)$ and $k^\xi E(k)$ in Fig. (2G) and Fig. (2H), respectively. In other words, our results clearly show that the wavenumber k_p depends non-monotonically on the Deborah number, being maximum for $\text{De} \approx 1$.

Although, the steepening of the spectra beyond a certain wavenumber $k = k_p$ have been observed before in both direct numerical simulations [9, 11, 18, 19, 27] and experiments [33], this was mostly confined to the dissipation range due to the small separation of scales related to the Reynolds number considered; only recent experiments [1], for the first time, demonstrated the emergence of this elastic scaling. Ref. [1] also found that L_p increases with the polymer concentration but they did not investigate how it behaves as a function of the Deborah number. Also, we, for the first time, find both Kolmogorov and elastic scaling simultaneously valid for different ranges of wavenumbers by virtue of running the largest simulation of polymeric turbulence so far and we also uncover the non-monotonic behavior of L_p as a function of the Deborah number.

The previous results have been obtained for the purely elastic Oldroyd-B model. Before we explore further the elastic scaling, it is worth mentioning that we performed the simulation for $\text{De} \approx 0.95$ with two additional models of polymeric fluids – the inelastic, shear-thinning Carreau Yasuda model and the FENE-P model which models both the elastic and shear-thinning behaviour of polymeric fluids. We find that the new scaling at intermediate scales is a purely elastic effect, which completely disappear in the absence of elasticity, while it is reduced when shear-thinning is present together with elasticity (see Fig. (Supplementary 2) in the Supplementary Materials).

D. Scale-by-scale energy budget

In turbulence, to understand the energy spectra we have to study the flux of energy through scales [45, 48, 49]. For polymeric turbulence, the flux in Fourier space

have been studied before by Refs. [26, 27] and their real space analog in Ref. [18]. To obtain the flux of kinetic energy in Fourier space, transform (1a) to Fourier space, multiply by $\hat{u}(-\mathbf{k})$, integrate over the solid angle $d\Omega$ and over k from 0 to K , and average over the statistically stationary state of turbulence to obtain

$$\partial_t \mathcal{E}(K) = \Pi_f(K) - \mathcal{D}_f(K) + \mathcal{P}(K) + \mathcal{F}_{\text{inj}}(K), \quad (6)$$

where $\mathcal{E}(K) = \int_0^K E(k)dk$, and Π_f , $-\mathcal{D}_f$, \mathcal{P} and \mathcal{F}_{inj} are the contributions from the nonlinear term, the viscous term, the polymeric stress and the external force in (1a). The contribution from the dissipative term, $-\mathcal{D}_f$, is always negative, while the contribution from the external force, \mathcal{F}_{inj} , is always positive. Since we consider a statistically stationary state, the left hand side of (6) is zero; for $K \gg k_{\text{inj}}$, the contribution from the external force \mathcal{F}_{inj} remains a constant, i.e., $\mathcal{F}_{\text{inj}}(K \gg k_{\text{inj}}) = \varepsilon_{\text{inj}}$. In the absence of polymers, $\mathcal{P} = 0$, and, since in the inertial range the dissipative contribution \mathcal{D}_f is negligible, $\Pi_f(K) = \varepsilon_{\text{inj}}$ is a constant.

The novel physics of this problem is elucidated by studying the contribution from the polymers, \mathcal{P} . In Fig. (3A) we show a representative plot of $\mathcal{P}(K)$ as a function of K , plotted as a dashed-dotted line. We arbitrarily divide this into two parts,

$$\mathcal{P}(K) = \Pi_p(K) - \mathcal{D}_p(K), \quad (7)$$

where we define

$$\mathcal{D}_p(K) = \frac{\varepsilon_p}{\varepsilon_f} \mathcal{D}_f(K). \quad (8)$$

In other words, we extract one part of $\mathcal{P}(K)$ which is a pure dissipative contribution, \mathcal{D}_p , because we know that one role played by this term is the increased dissipation in addition to the fluid dissipation. We plot Π_p and \mathcal{D}_p individually in Fig. (3A). Remarkably, Π_p has the same qualitative behavior as Π_f , the nonlinear flux. In Fig. (3B) we plot both Π_p and Π_f denoted by the symbol $+$ and a continuous line respectively. We find that for small K , Π_f is dominant and Π_p is insignificant. At a certain scale k_* the two fluxes cross each other. Beyond k_* , Π_p is the dominant partner and Π_f is negligible. At very large K , well within the dissipation range, both Π_f and Π_p go to zero. The sum of these two fluxes $\Pi \equiv \Pi_p + \Pi_f$ is practically a constant for all $K \ll k_\eta$. In the same figure, Fig. (3B), we also plot, as a black line, the contribution to the flux from the nonlinear term for a simulation with no polymers. Clearly, the flux that is carried by the nonlinear term in the absence of polymers is carried by both Π_f and Π_p in the presence of polymers: at small K the flux is carried solely by Π_f and at large K the flux is carried solely by Π_p . The crossover between this two fluxes happens at k_* which we identify with k_p . The fluxes clearly illustrate and substantiate what we already observed in the energy spectra: for $k < k_p$ the turbulence is Kolmogorov-like whereas for $k_p < k < k_\eta$ the polymeric flux Π_p dominates and is approximately a constant. We define the range of Fourier

modes, $k_p < k < k_\eta$ as the *elastic range* with k_p precisely defined as $\Pi_f(k_p) = \Pi_p(k_p)$.

For a moment, again consider turbulence without polymers. Assume that within the inertial range, in real space, the velocity shows scaling behavior with an exponent h such that, if we scale length by a factor of b , $x \rightarrow bx$, then velocity scales as $u \rightarrow b^h u$. In the inertial range, the flux equation, (6), implies that the contribution to the flux from the nonlinear term is constant, $\Pi_f = \text{constant}$. Applying simple power-counting to the contribution to the flux from the nonlinear term, we obtain $3h - 1 = 0$, which implies the standard result from Kolmogorov theory $h = 1/3$. Let us now apply the same scaling argument to the elastic range. As we scale $x \rightarrow bx$, we expect $u \rightarrow b^h u$, and $C \rightarrow b^g C$ with two distinct exponents h and g , respectively. As the flux Π_p is constant in the elastic range, we obtain $h - 1 + g = 0$. By Fourier transform, it is straightforward to show that, if the velocity in real space scales with an exponent h , then the scaling exponent for the energy, $E(k) \sim k^{-\xi}$, with $\xi = 2h + 1$. Together the two relations imply that the scaling exponent for the shell-integrated polymer energy is $E_p(k) \sim k^{-\psi}$, with $\psi = g + 1 = 2 - (\xi - 1)/2 \approx 1.35$. In Fig. (2I) we plot the compensated shell-integrated polymer spectra from our simulations; a scaling exponent of $\psi \approx 1.35$ is indeed consistent with our results corroborating the view of a polymer flux.

Next, we show how the flux-balance depends on the Deborah number in Fig. (3C) to Fig. (3H). We mark two Fourier modes in these plots, one is k_p , marked by a black circle, and the other is the crossover between Π and \mathcal{D}_f , which is a reasonable estimate of k_η , marked by a black square. For small De, Fig. (3C), $k_p > k_\eta$; in other words, the elastic range is non-existent – masked by the viscous range. As De increases, Fig. (3D) to Fig. (3E), $k_p < k_\eta$ and the elastic range is clearly visible, with k_p reducing with De. As De increases beyond unity, k_p starts increasing again, Fig. (3F), and becomes almost equal to k_η in Fig. (3G). For even larger De the elastic range disappears again.

Finally, this non-monotonic behavior of the scale k_p is also reflected in the probability distribution function (PDF) of the extension of the polymers, $\text{Tr}(\mathcal{C})$, shown in Fig. (4) for the Oldroyd-B model. For small De, the PDF has a peak somewhat higher than 3, i.e., some polymers are already not in a coiled state. This is expected because the stretching of polymers is determined by the small scale strain-rate [50–52] which is best captured by the Weissenberg number, which is about 16 for the smallest Deborah number we used. As De is increased, the peak of the PDF moves to higher and higher values, which is also what is expected. Surprisingly, for $\text{De} > 1$ the peak again moves back to smaller values. This is an effect that cannot be captured from a passive polymer theory [47] – the feedback from the polymer to the flow changes the strain-rate such that in turn the stretching of the polymers is reversed at Deborah number greater than unity. Note that here we show results from the Oldroyd-B model

where there is no constraint on the maximum stretching of polymers; however, this non-monotonic behaviour is not unique to the Oldroyd-B model, it is also seen in FENE-P (see Fig. (Supplementary 3) in the Supplementary Materials).

To summarize, we have, so far, presented evidence from the largest resolution direct numerical simulations of polymeric turbulence that, if the Deborah number lies in the right range, $k_p < k < k_\eta$, an elastic range with constant polymeric flux Π_p emerges in which $E(k) \sim k^{-\xi}$, with $\xi \approx 2.3$ and $E_p(k) \sim k^{-\psi}$ with $\psi \approx 1.35$. Crucially, the scale k_p behaves non-monotonically as a function of De and can be precisely determined as the crossover scale between Π_f and Π_p .

E. Structure function and intermittency

In the absence of polymers, the scaling exponents of the structure function ζ_q is a nonlinear function of q – a phenomena known as intermittency. We now explore what happens to intermittency within the elastic range. In Fig. (5A) we plot the structure function for $q = 2, 4$, and 6 for $\text{De} \approx 0.9$ – the case for which we have the largest elastic range. The second order structure function, (3b) with $q = 2$, is the Fourier transform of the energy spectrum $E(k)$. Hence, if $E(k) \sim k^{-\xi}$, then $S_2(\ell) \sim \ell^{\zeta_2}$, with $\zeta_2 = \xi - 1 \approx 1.3$ – which is what we obtain. On the other hand, the scalings for $q = 4$ and $q = 6$ are different from $2\zeta_2$ and $3\zeta_2$. This becomes obvious when we plot in Fig. (5B) S_4 and S_6 as a function of S_2 . In these plots the elastic range and the inertial range seems to merge into one scaling range, suggesting that the intermittency correction for $q = 4$ and $q = 6$ are the same in both the elastic and the inertial range. The extension of the scaling range of the structure functions in Fig. (5B) is reminiscent of the well-known phenomena of extended self-similarity [53] observed in Newtonian turbulence. Our results on intermittency agrees with and extend the experimental results obtained in Ref. [1]. We note that, since higher order structure function are higher order moments of the probability distribution function of the velocity difference, they are less accurately known compared to the second order one. In other words, the exponents ζ_4 and ζ_6 are known less accurately than ζ_2 . Hence, the conclusion that the intermittency corrections are the same in both elastic and inertial range must be treated with caution. If indeed, this conclusion is further confirmed by future work, this would be a remarkable result for the following reason: at this moment we do not have a theory of intermittency, however we do know that it depends sensitively on the cascade determined by the nonlinear term[54]. The same intermittency correction in the elastic and inertial range would imply that the elastic term mimics closely the inertial one.

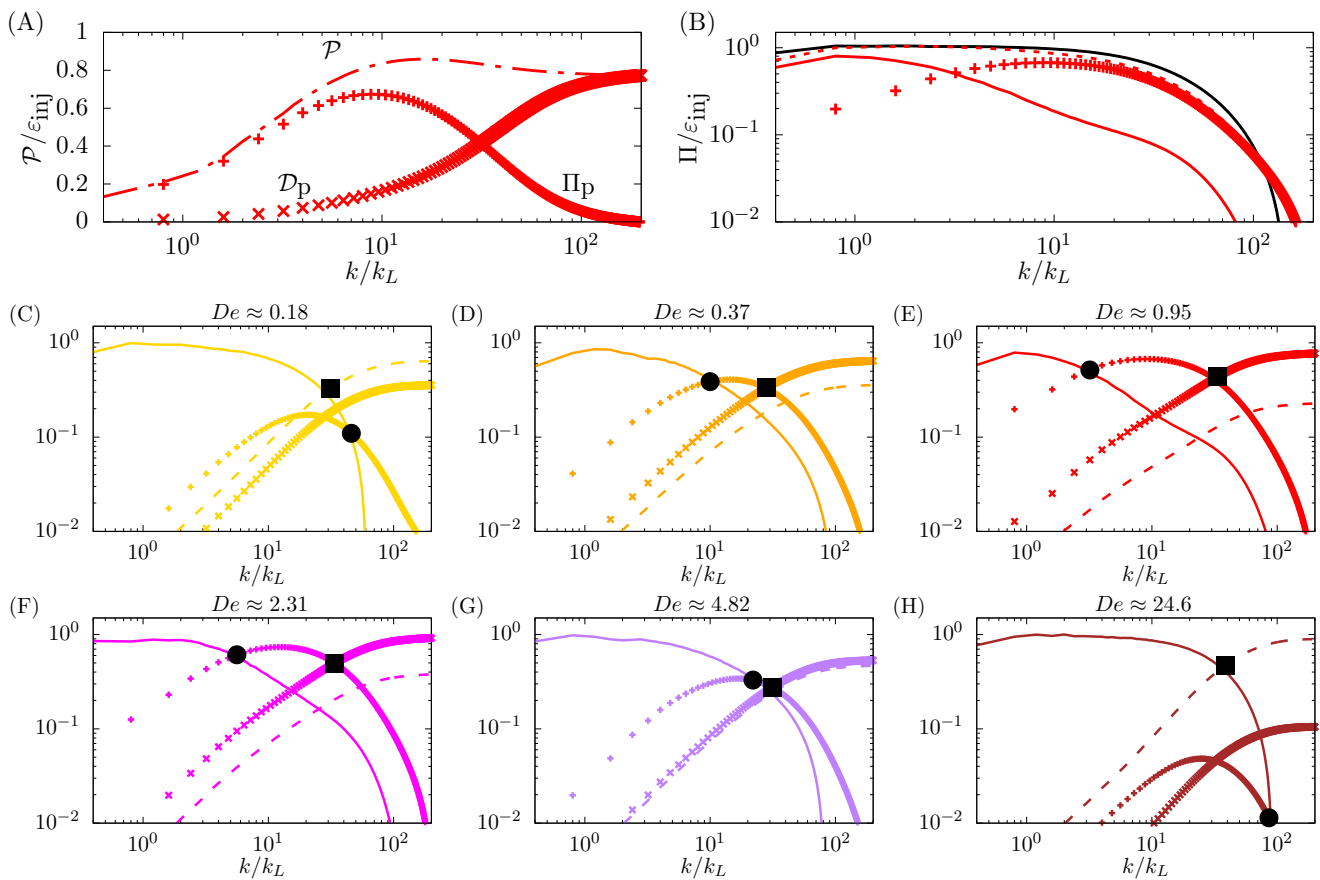


FIG. 3. **Scale by scale energy budget** (A): The polymer contribution to the spectral energy balance, \mathcal{P} , (dash-dotted line) is decomposed into a (\times) pure polymer dissipation term, \mathcal{D}_p and a (+) pure polymer energy flux, Π_p , see (7). (B): The sum of the (solid line) non-linear energy flux Π_f and of the (+) polymer flux Π_p provide a (dotted line) total flux $\Pi = \Pi_f + \Pi_p$ extending over a range comparable to the Newtonian case (black line). (C) to (H): The panels show the non-linear energy flux Π_f (solid line), fluid dissipation \mathcal{D}_f (dashed line), polymer flux, Π_p (+), and polymer dissipation \mathcal{D}_p (\times) for different Deborah numbers. The filled circles represent k_p and the filled squares k_η . As De approaches unity, the polymer flux and dissipation grow, while they decrease for larger values.

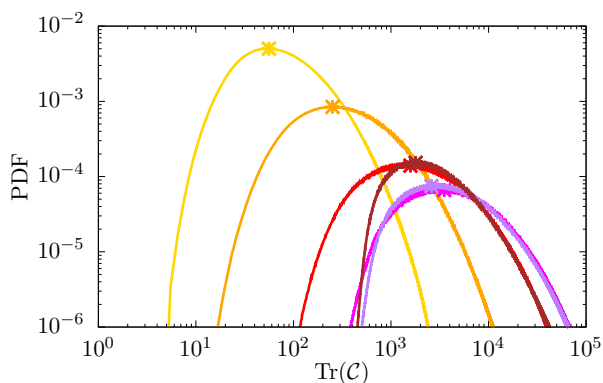


FIG. 4. **Polymer extension.** Probability distribution function (PDF) of the polymer extension for different Deborah numbers, measured in terms of $\text{Tr}(C)$.

III. CONCLUSION AND OUTLOOK

Our simulations reach the highest Re and De numbers reached so far in numerical simulations of homogeneous and isotropic turbulence of polymer solutions [55]. Hence, by modern nomenclature, we may call this *elasto-inertial turbulence* [27, 56], which is merely a renaming of the traditional field of polymeric turbulence. We find that the central role of the polymers is that the cascade of energy, which in absence of polymers is determined by the advective nonlinearity, is now carried by both the advective nonlinearity and the polymer stress *but at different scales*. At large scales, the energy flux through scales is dominated by the advective nonlinearity, while the polymer stress plays a sub-dominant role – this is reversed at smaller scales. This gives rise to two scaling ranges, the classical Kolmogorov one and the new elastic one. We emphasize that the new scaling we find is a purely elastic effect, the advective nonlinearity plays a sub-dominant role in the range of scales where the elastic

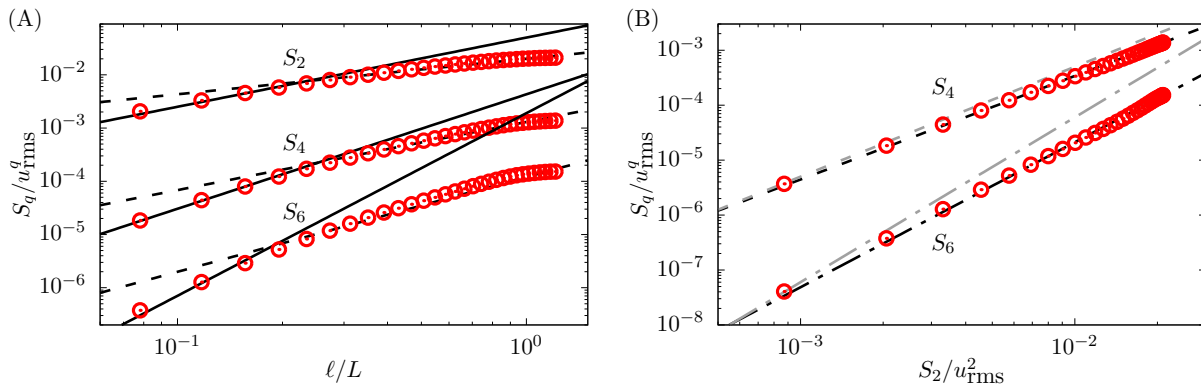


FIG. 5. **Structure functions and intermittency.** (A): Structure function S_q for $q = 2, 4$ and 6 from top to bottom for the viscoelastic case at $De \approx 0.9$. The solid and dashed lines represent the expected scalings in the polymer and inertial range of scales, corrected by the intermittency correction. (B): Same structure functions of the panel (A), plotted in their Extended Self Similarity form. The black and gray lines represent the expected scaling with and without intermittency corrections. The polymer and inertial range of scales follows the same line, indicating that the intermittency in the two ranges is the same.

scaling is observed. Thus elasto-inertial turbulence appears to be inertial turbulence at large scale and a new elastic behaviour – different from elastic turbulence – at smaller scales which are still larger than viscous scales. The viscous effects may dominate over the elastic effects for small Re , thereby making the elastic range disappear. Furthermore, we establish that this elastic behaviour is non-monotonic in Deborah number – it cannot be captured by a theory that treats polymers as passive objects. The scaling exponent we observed is consistent with what has been observed in recent experiments [1] which did not probe the Deborah number dependence of their results.

At present there are no theories that help us understand the novel scaling. To the best of our knowledge the first theory that predicted a new power-law scaling in elastic range is by Bhattacharjee and Thirumalai [13, 14], whose theory gives an exponent of $\xi = 3$ in the elastic range; by contrast we observe $\xi \approx 2.3$, consistent with re-

cent experiments [1]. Bhattacharjee and Thirumalai also assumed that most of the polymers have not undergone coil-stretch transition. In our simulations, this may be true at small De , where the elastic range is non-existent, but this is definitely not the case at high De where we do observe the elastic scaling. The theory by Fouxon and Lebedev [15] also predicts a power-law scaling ($\xi > 3$) and the existence of an elastic range, but we agree with Zhang et al [1] that “the assumptions and quantitative prediction of the theory are not supported by” our numerics. Our simulations measure quantities that are not easily accessible in the experiments, e.g., the contribution from the polymeric stress and the PDF of polymer extension, thus proving constraints and clues to a future theory.

IV. REFERENCES AND NOTES

- [1] Yi-Bao Zhang, Eberhard Bodenschatz, Haitao Xu, and Heng-Dong Xi, “Experimental observation of the elastic range scaling in turbulent flow with polymer additives,” *Science Advances* **7**, eabd3525 (2021).
- [2] B. Toms, in *Proceedings of First International Congress on Rheology Volume II* (North-Holland, Amsterdam, 1949) pp. 135.
- [3] M. Tabor and P.G. De Gennes, “A cascade theory of drag reduction,” *Europhys. Lett.* **2**, 519–522 (1986).
- [4] E.J. Hinch, “Mechanical models of dilute polymer solution in strong flows,” *Phys. Fluids*. **20**, S22 (1977).
- [5] J.L. Lumley, “Drag reduction in turbulent flow by polymer additives,” *J. Polymer Sci* **7**, 263–290 (1973).
- [6] D. Bonn, Y. Couder, P.H.J. van Dam, and S. Douady, “From small scales to large scales in three-dimensional turbulence: The effect of diluted polymers,” *Phys. Rev. E* **47**, R28 (1993).
- [7] Eric van Doorn, Christopher M White, and KR Sreenivasan, “The decay of grid turbulence in polymer and surfactant solutions,” *Physics of Fluids* **11**, 2387–2393 (1999).
- [8] C Kalelkar, R Govindarajan, and R Pandit, “Drag reduction by polymer additives in decaying turbulence,” *Phys. Rev. E* **72**, 017301 (2004).
- [9] Prasad Perlekar, Dhruvadya Mitra, and Rahul Pandit, “Manifestations of drag reduction by polymer additives in decaying, homogeneous, isotropic turbulence,” *Phys. Rev. Lett.* **97**, 264501 (2006).
- [10] P. Perlekar, *Numerical Studies of three dimensional turbulence with polymer additives and two dimensional turbulence in thin films.*, Ph.D. thesis, Indian Institute of Science, Bangalore, India (2009).
- [11] Prasad Perlekar, Dhruvadya Mitra, and Rahul Pandit, “Direct numerical simulations of statistically steady, ho-

- homogeneous, isotropic fluid turbulence with polymer additives,” *Phys. Rev. E* **82**, 066313 (2010).
- [12] W-H Cai, F-C Li, and H-N Zhang, “Dns study of decaying homogeneous isotropic turbulence with polymer additives,” *Journal of Fluid Mechanics* **665**, 334–356 (2010).
- [13] JK Bhattacharjee and D Thirumalai, “Drag reduction in turbulent flows by polymers,” *Physical review letters* **67**, 196 (1991).
- [14] D Thirumalai and JK Bhattacharjee, “Polymer-induced drag reduction in turbulent flows,” *Physical Review E* **53**, 546 (1996).
- [15] A. Fouxon and V. Lebedev, “Spectra of turbulence in dilute polymer solutions,” *Phys. Fluids*. **15**, 2060 (2003).
- [16] T. Vaithianathan and L.R. Collins, “Numerical approach to simulating turbulent flow of a viscoelastic polymer solution,” *Journal of Computational Physics* **187**, 1–21 (2003).
- [17] R. Benzi, E. De Angelis, R. Govindarajan, and I. Procaccia, “Shell model for drag reduction with polymer additives in homogeneous turbulence,” *Phys. Rev. E* **68**, 016308 (2003).
- [18] E De Angelis, CM Casciola, R Benzi, and R Piva, “Homogeneous isotropic turbulence in dilute polymers,” *Journal of Fluid Mechanics* **531**, 1–10 (2005).
- [19] S Berti, A Bistagnino, Guido Boffetta, A Celani, and S Musacchio, “Small-scale statistics of viscoelastic turbulence,” *EPL (Europhysics Letters)* **76**, 63 (2006).
- [20] T. Peters and J. Schumacher, “Two-way coupling of fene dumbbells with a turbulent shear flow.” *Phys. Fluids* **19**, 065109 (2007).
- [21] Filippo De Lillo, Guido Boffetta, and Stefano Musacchio, “Control of particle clustering in turbulence by polymer additives,” *Physical Review E* **85**, 036308 (2012).
- [22] Takeshi Watanabe and Toshiyuki Gotoh, “Hybrid eulerian–lagrangian simulations for polymer–turbulence interactions,” *Journal of Fluid Mechanics* **717**, 535–575 (2013).
- [23] Mani Fathali and Saber Khoei, “Spectral energy transfer in a viscoelastic homogeneous isotropic turbulence,” *Physics of Fluids* **31**, 095105 (2019).
- [24] Takeshi Watanabe and Toshiyuki Gotoh, “Power-law spectra formed by stretching polymers in decaying isotropic turbulence,” *Physics of Fluids* **26**, 035110 (2014).
- [25] M Quan Nguyen, Alexandre Delache, Serge Simoëns, Wouter JT Bos, and Mamoud El Hajem, “Small scale dynamics of isotropic viscoelastic turbulence,” *Physical Review Fluids* **1**, 083301 (2016).
- [26] PC Valente, CB Da Silva, and FT Pinho, “The effect of viscoelasticity on the turbulent kinetic energy cascade,” *Journal of fluid mechanics* **760**, 39–62 (2014).
- [27] PC Valente, CB da Silva, and FT Pinho, “Energy spectra in elasto-inertial turbulence,” *Physics of Fluids* **28**, 075108 (2016).
- [28] C. Friehe and W. Schwarz, *J. Fluid. Mech* **44**, 173 (1970).
- [29] W. McComb, J. Allan, and C. Greated, *Phys. Fluid* **20**, 873 (1977).
- [30] D. Bonn, Y. Amarouchene, C. Wagner, S. Douady, and O. Cadot, “Turbulent drag reduction by polymers,” *J. Phys. CM* **17**, S1219 (2005).
- [31] A. Liberzon, M. Guala, W. Kinzelbach, and A. Tsinober, *Phys. Fluids*. **18**, 125101 (2006).
- [32] N.T. Ouellette, H. Xu, and E. Bodenschatz, “Bulk turbulence in dilute polymer solutions,” *J. Fluid Mech.* **629**, 375–385 (2009).
- [33] Richard Vonlanthen and Peter A Monkewitz, “Grid turbulence in dilute polymer solutions: Peo in water,” *Journal of Fluid Mechanics* **730**, 76–98 (2013).
- [34] LD Landau and EM Lifshitz, *Fluid mechanics*, Course of Theoretical Physics, Vol. 6 (Pergamon Press Ltd., Oxford, England, 1959).
- [35] Alexander Groisman and Victor Steinberg, “Elastic turbulence in a polymer solution,” *Nature* **405**, 53 (2000).
- [36] Victor Steinberg, “Elastic turbulence: an experimental view on inertialess random flow,” *Annual Review of Fluid Mechanics* **53**, 27–58 (2021).
- [37] Heng-Dong Xi, Eberhard Bodenschatz, and Haitao Xu, “Elastic energy flux by flexible polymers in fluid turbulence,” *Physical review letters* **111**, 024501 (2013).
- [38] John L Lumley, “Drag reduction by additives,” *Annual review of fluid mechanics* **1**, 367–384 (1969).
- [39] A. Peterlin, *J. Polym. Sci., Polym. Lett.* **4**, 287 (1966).
- [40] H. Warner, *Ind. Eng. Chem. Fundamentals* **11**, 379 (1972).
- [41] R. Armstrong, *J. Chem. Phys.* **60**, 724 (1974).
- [42] R. Bird, C. Curtiss, R. Armstrong, and O. Hassager, *Dynamics of Polymeric Liquids* (Wiley, New York, 1987).
- [43] N. Phan-Thien, *Understanding Viscoelasticity* (Springer, Berlin, 2002).
- [44] Vinayak Eswaran and Stephen B Pope, “An examination of forcing in direct numerical simulations of turbulence,” *Computers & Fluids* **16**, 257–278 (1988).
- [45] U. Frisch, *Turbulence the legacy of A.N. Kolmogorov* (Cambridge University Press, Cambridge, 1996).
- [46] Nusret Balci, Becca Thomases, Michael Renardy, and Charles R Doering, “Symmetric factorization of the conformation tensor in viscoelastic fluid models,” *Journal of Non-Newtonian Fluid Mechanics* **166**, 546–553 (2011).
- [47] R. Benzi and E.S.C. Ching, *Rev. Mod. Phys.* **9**, 163 (2018).
- [48] S.B. Pope, *Turbulence* (Cambridge University Press, Cambridge, 2000).
- [49] Mahendra K Verma, *Energy transfers in fluid flows: multiscale and spectral perspectives* (Cambridge University Press, 2019).
- [50] Michael Chertkov, “Polymer stretching by turbulence,” *Physical review letters* **84**, 4761 (2000).
- [51] M Martins Afonso and D Vincenzi, “Nonlinear elastic polymers in random flow,” *Journal of Fluid Mechanics* **540**, 99–108 (2005).
- [52] Stefano Musacchio and Dario Vincenzi, “Deformation of a flexible polymer in a random flow with long correlation time,” *Journal of fluid mechanics* **670**, 326–336 (2011).
- [53] R. Benzi, S. Ciliberto, R. Trippiccone, C. Baudet, F. Massaioli, and S. Succi, *Phys. Rev E* **48**, R29 (1993).
- [54] Ganapati Sahoo and Luca Biferale, “Energy cascade and intermittency in helically decomposed navier–stokes equations,” *Fluid Dynamics Research* **50**, 011420 (2018).
- [55] See supplemental material for a comparisons of our parameters with all earlier simulations.
- [56] Devranjan Samanta, Yves Dubief, Markus Holzner, Christof Schäfer, Alexander N Morozov, Christian Wagner, and Björn Hof, “Elasto-inertial turbulence,” *Proceedings of the National Academy of Sciences* **110**, 10557–10562 (2013).
- [57] M. E. Rosti, Z. Ge, S. S. Jain, M. S. Dodd, and L. Brandt, “Droplets in homogeneous shear turbulence,” *J. Fluid Mech.* **876**, 962–984 (2019).

- [58] M. E. Rosti and L. Brandt, “Increase of turbulent drag by polymers in particle suspensions,” *Phys. Rev. Fluids* **5**, 041301 (2020).
- [59] M. E. Rosti, S. Olivieri, M. Cavaiola, A. Seminara, and A. Mazzino, “Fluid dynamics of COVID-19 airborne infection suggests urgent data for a scientific design of social distancing,” *Sci. Rep.* **10**, 1–9 (2020).
- [60] S. Olivieri, L. Brandt, M. E. Rosti, and A. Mazzino, “Dispersed fibers change the classical energy budget of turbulence via nonlocal transfer,” *Phys. Rev. Lett.* **125**, 114501 (2020).
- [61] M. E. Rosti, M. Cavaiola, S. Olivieri, A. Seminara, and A. Mazzino, “Turbulence role in the fate of virus-containing droplets in violent expiratory events,” *Phys. Rev. Research* **3**, 013091 (2021).
- [62] A. Mazzino and M. E. Rosti, “Unraveling the secrets of turbulence in a fluid puff,” *Physical Review Letters* **127**, 094501 (2021).
- [63] S. Brizzolara, M. E. Rosti, S. Olivieri, L. Brandt, M. Holzner, and A. Mazzino, “Fiber tracking velocimetry for two-point statistics of turbulence,” *Phys. Rev. X* **11**, 031060 (2021).
- [64] R. Fattal and R. Kupferman, “Constitutive laws for the matrix-logarithm of the conformation tensor,” *Journal of Non-Newtonian Fluid Mechanics* **123**, 281–285 (2004).

V. ACKNOWLEDGMENTS

M.E.R. thanks Ms. Megumi Ikeda of the Complex Fluids and Flows unit at OIST for the help and useful discussions in preparing the flow visualisation.

A. Funding

M.E.R. is supported by the Okinawa Institute of Science and Technology Graduate University (OIST) with subsidy funding from the Cabinet Office, Government of Japan. M.E.R. also acknowledges the computational time provided by HPCI on the Fugaku cluster under the grant hp210229 and the computer time provided by the Scientific Computing section of Research Support Division at OIST. PP acknowledges support from the Department of Atomic Energy (DAE), India under Project Identification No. RTI 4007, and DST (India) Project Nos. ECR/2018/001135 and DST/NSM/R&D_HPC_Applications/2021/29. DM acknowledges the support of the Swedish Research Council Grant No. 638-2013-9243 and 2016-05225.

B. Author contributions

M.E.R. conceived the original idea, planned the research, developed the code and performed the numerical simulations. All authors analyzed data, outlined the manuscript content and wrote the manuscript.

C. Competing interests

The authors declare that they have no competing interests.

D. Data and materials availability

All data needed to evaluate the conclusions are present in the paper and/or the Supplementary Materials. Additional data related to this work may be requested from the authors.

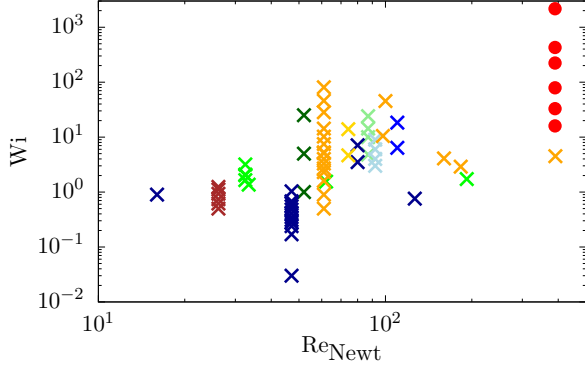


FIG. Supplementary 1. **DNS data of polymeric turbulence available in the literature.** The plot reports the reference Reynolds numbers of the Newtonian cases Re_{Newt} and the Weissenberg numbers Wi of the simulations available in the literature: the cross symbols represents the previous investigations, while the filled circles the present one. Light green: [19]; green: [25]; dark-green: [22, 24]; light blue: [23]; blue: [21]; dark blue: [9, 11]; orange: [26, 27]; gold: [18]; brown: [12]. The results of the present work focus on a high Re and Wi region never investigated before.

SUPPLEMENTARY INFORMATION

Materials and methods

The viscoelastic fluid is governed by the conservation of momentum and the incompressibility constraint:

$$\rho_f \left(\frac{\partial u_\alpha}{\partial t} + \frac{\partial u_\alpha u_\beta}{\partial x_\beta} \right) = -\frac{\partial p}{\partial x_\alpha} + \frac{\partial}{\partial x_\beta} \left(2\mu_f S_{\alpha\beta} + \frac{\mu_p}{\tau_p} f C_{\alpha\beta} \right), \quad (9a)$$

$$\frac{\partial u_\alpha}{\partial x_\alpha} = 0. \quad (9b)$$

In the previous set of equations, ρ_f and μ_f are the density and dynamic viscosity of the fluid, p is the pressure, and \mathcal{S} the rate-of-strain tensor with components $S_{\alpha\beta}$ defined as $S_{\alpha\beta} = (\partial u_\alpha / \partial x_\beta + \partial u_\beta / \partial x_\alpha) / 2$. The last term in the momentum equation is the non-Newtonian contribution, with μ_p being the polymer viscosity, τ_p the polymer relaxation time, f a scalar function and \mathcal{C} the conformation tensor with components $C_{\alpha\beta}$ found by solving the

following transport equation:

$$\frac{\partial C_{\alpha\beta}}{\partial t} + u_\beta \frac{\partial C_{\alpha\beta}}{\partial x_\beta} = C_{\alpha\gamma} \frac{\partial u_\beta}{\partial x_\gamma} + C_{\gamma\beta} \frac{\partial u_\gamma}{\partial x_\alpha} - \frac{f C_{\alpha\beta} - \delta_{\alpha\beta}}{\tau_p}. \quad (10)$$

The function f is equal to $f = 1$ in the purely elastic Oldroyd-B model, and to $f = (\mathcal{L}^2 - 3) / (\mathcal{L}^2 - C_{\gamma\gamma})$ in the FENE-P model (\mathcal{L} is the maximum polymer extensibility) exhibiting both shear-thinning and elasticity. Turbulence is sustained by an additional forcing in the momentum equation; in particular, we use the spectral scheme by Eswaran and Pope [44] to randomly injecting energy within a low-wavenumber shell with $1 \leq k \leq 2$.

The equations of motion are solved numerically within a periodic cubic domain box of length 2π , discretized with $N = 1024$ grid points per side with a uniform spacing in all directions, resulting in a total number of around 1 billion grid points. The grid resolution used in the present work is the largest used for viscoelastic fluids and is sufficient to represent all the relevant quantities of interest ($k_{\text{max}}\eta \approx 1.7$). To solve the problem, we use the flow solver *Fujin*, an in-house code, extensively validated and used in a variety of problems [57–63], based on the (second-order) finite-difference method for the spatial discretization and the (second-order) Adams-Bashforth scheme for time marching. See also <https://groups.oist.jp/cffu/code> for a list of validations. The non-Newtonian stress equation is solved following the log-conformation approach [64] to ensure the positive-definiteness of the tensor even at high De .

Elasticity and shear-thinning

We consider three different models of polymeric fluids: the Oldroyd-B model (elasticity), the FENE-P model (elasticity and shear-thinning), and the Carreau–Yasuda model (shear-thinning), see Tab. Supplementary 1 for the full list of simulations performed. In the inelastic shear-thinning fluid, the fluid viscosity μ_f is a function of the local shear rate $\dot{\gamma}$ as

$$\frac{\mu}{\mu_0} = \frac{\mu_\infty}{\mu_0} + \left(1 - \frac{\mu_\infty}{\mu_0} \right) \left[1 + (\tau_p \dot{\gamma})^2 \right]^{\left(\frac{n-1}{2} \right)}, \quad (11)$$

where μ_0 and μ_∞ are the viscosity at zero and infinite shear rates, n is the power index ($n = 0.4$) and τ_p the consistency index. The model parameters are found to fit the FENE-P shear-thinning rheology, as shown in the inset of Fig. (Supplementary 2).

TABLE Supplementary 1. List of cases considered in the present work.

case	model	Re_λ	De	Wi	$\mu_p/(\mu_p + \mu_f)$	\mathcal{L}
○	single phase	390	—	—	0.1	—
◇	Oldroyd-B	480	0.18	16	0.1	∞
◇	Oldroyd-B	630	0.37	33	0.1	∞
○	Oldroyd-B	740	0.95	79	0.1	∞
△	Oldroyd-B	690	2.31	223	0.1	∞
▽	Oldroyd-B	614	4.82	427	0.1	∞
□	Oldroyd-B	447	24.6	2169	0.1	∞
○	FENE-P	610	0.85	31	0.1	60
○	Carreau-Yasuda	370	—	—	—	—

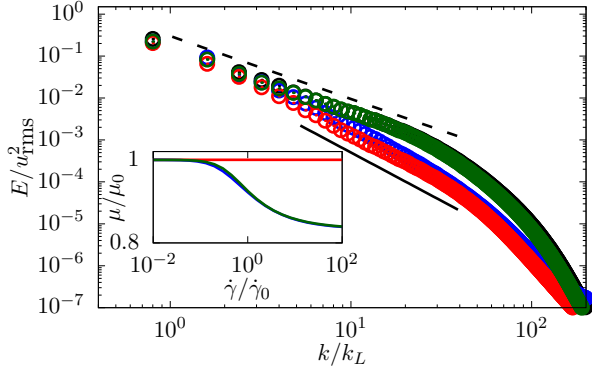


FIG. Supplementary 2. **Effect of shear-thinning and elasticity.** Energy spectra for $De \approx 0.95$ for different fluids. Black: Newtonian fluid. Green: inelastic Carreau Yasuda model. Blue: FENE-P model. Red: Oldroyd-B model. The inset shows the shear rheology of the same fluids. The new scaling at intermediate small scales is a purely elastic effect, which completely disappear in the absence of elasticity while it is reduced when shear-thinning is present together with elasticity. The dashed and solid lines represent the scaling $k^{-\psi}$ with $\psi = 5/3$ and $\psi \approx 1.35$.

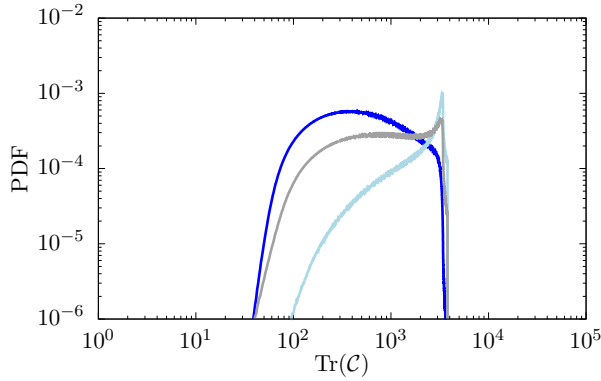


FIG. Supplementary 3. **Polymer extension.** Probability distribution function (PDF) of the polymer extension for different Deborah numbers, measured in terms of $\text{Tr}(\mathcal{C})$, obtained with the FENE-P model. Blue: $De \approx 0.95$; light blue: $De \approx 2.31$; gray: $De \approx 4.82$. Differently from the results obtained with the Oldroyd-B model, the polymer extension is upper bounded by \mathcal{L}^2 ; however, the non-monotonic trend with De is still evident.